Electrochemical, Magnetic, and Electrical Properties of α,ω-Capped Sexithiophene Films. 2. Conduction in Sexithiophenes with α,ω-Aryl-Extended Conjugation

G. Zotti,* S. Zecchin, and B. Vercelli

Istituto CNR per l'Energetica e le Interfasi, c.o Stati Uniti 4, 35127 Padova, Italy

M. Pasini, S. Destri, and F. Bertini

Istituto CNR per lo Studio delle Macromolecole, via E.Bassini 15, 20133 Milano, Italy

A. Berlin

Istituto CNR di Scienze e Tecnologie Molecolari, via C.Golgi 19, 20133 Milano, Italy

Received March 21, 2006. Revised Manuscript Received April 27, 2006

Thin films of tetrahexylsexithiophenes, fluorenonyl- and fluorenyl-protected at the terminal α,ω-positions, were investigated by cyclic voltammetry, electrochemical quartz crystal microbalance analysis, in situ ESR, and in situ conductivity. Reversible oxidation is composed of three separate steps, two one-electron processes and a further multielectron process. ESR indicates strong magnetic dimerization for the one-electron-oxidized species. Conductivity is redox type at the cation−dication (polaron−bipolaron) state and metal-like at doping levels higher than the bipolaron with a 20-fold increase at full oxidation. Hexyl-substituted α,ω-capped octathiophene, decathiophene, and dodecathiophene films have been similarly investigated to compare the effects of fluorenonyl and fluorenyl extension of sexithiophene with those given by additional thiophene rings. The conductivity, which increases progressively (by 3 orders of magnitude) with the oligothiophene chain length, is metal-like. In dodecathiophene the doping charge increases markedly, approaching four electrons per molecule, and the conductivity, maximized at the two-electron level, decreases linearly, approaching zero at the four-electron level. A bipolaron model of conductivity accounts for conductivity in oligothiophenes.

Introduction

Conjugated oligomers are highly interesting for the fabrication of plastic electronic devices[1] such as organic thin-film field-effect transistors (OFETs).[2] In particular, oligothiophenes[3] are good for such applications because of their excellent electronic properties, stability under ambient conditions, and ease of chemical modification.

Moreover, in light of recent molecular electronics, symmetrical conjugated molecular wires with two identical handles are actually investigated as model systems for molecular conduction,[4] and oligothiophenes are in this respect an interesting case.

Therefore, understanding the basic conductivity of these materials is of fundamental importance not only for the evaluation of their ability to charge transport in electronic devices but also for the analysis of the conductive properties of conjugated molecular wires. It is clear that whereas conduction operating in OFETs is that of low doping levels, the characteristics of molecular wires may be extended to include the whole available range of doping.

To clarify the factors affecting the conductive properties of such materials, we have previously investigated a series of newly synthesized α,ω-capped sexithiophenes in which the capping moieties differed in electron donor−acceptor properties.[5]

The purpose of this investigation is to evaluate the electronic (electrochemical, magnetic, and conductive) properties of α,ω-capped sexithiophenes when the conjugation is significantly extended. This has been accomplished using fluorene and fluorenone caps (Chart 1). In fact, a very large amount of research has been devoted to copolymers of thiophene and fluorene for OLED applications.[6] Moreover, alkyl chain end-capped oligofluorene−thiophenes have given highly ordered and stable polycrystalline films with charge carrier mobility as high as 0.1 $cm^2 V^{-1} s^{-1}$.[7] Furthermore, a paper has recently described a regular thiophene−fluorenone copolymer[8a] which has been used for the construction of an

* To whom correspondence should be addressed. Phone: (+39)49-8295868. Fax: (+39)49-8295853. E-mail: g.zotti@ieni.cnr.it.

(1) Special Issue on Organic Electronics. *Chem. Mater.* **2004**, *16*, 4381−4846.

(2) Dimitrakopoulos, C. D.; Malenfant, P. R. L. *Adv. Mater.* **2002**, *14*, 99. Katz, H.; Bao, Z.; Gilat, S. *Acc. Chem. Res.* **2001**, *34*, 359.

(3) Kline, R. J.; McGehee, M. D.; Kadnikova, E. N.; Liu, J.; Frechet, J. M. J. *Adv. Mater.* **2003**, *15*, 1519.

(4) (a) Carroll, R. L.; Gorman, C. B. *Angew. Chem., Int. Ed.* **2002**, *41*, 4379. (b) Salomon, A.; Cahen, D.; Lindsay, S.; Tomfohr, J.; Engelkes, V. B.; Frisbie, C. D. *Adv. Mater.* **2003**, *15*, 1881. (c) Metzger, R. M. *Chem. Rev.* **2003**, *103*, 3803. (d) James, D. K.; Tour, J. M. *Chem. Mater.* **2004,** *16*, 4423. (e) McCreery, R. L. *Chem. Mater.* **2004,** *16*, 4477.

(5) Zotti, G.; Zecchin, S.; Vercelli, B.; Berlin, A.; Grimoldi, S.; Pasini, M. C.; Raposo, M. M. M. *Chem. Mater.* **2005**, *17*, 6492.

10.1021/cm060671h CCC: $33.50
Published on Web 05/28/2006

Chart 1

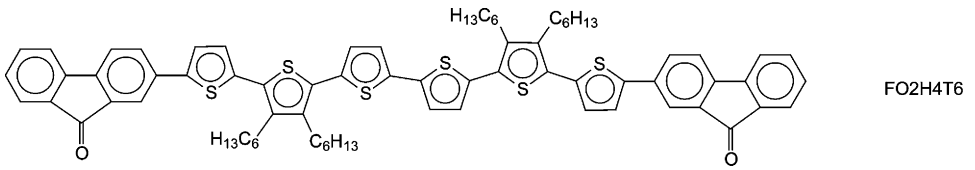

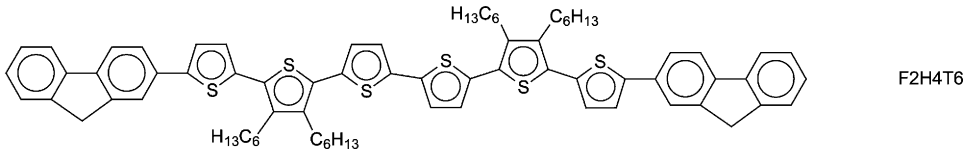

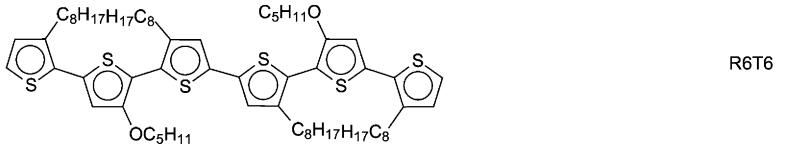

Chart 2

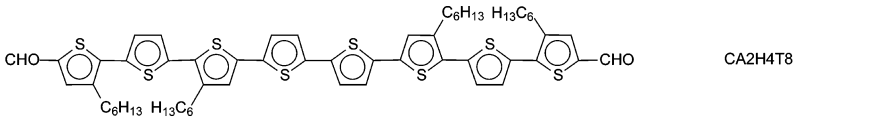

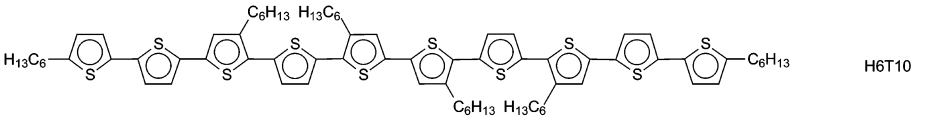

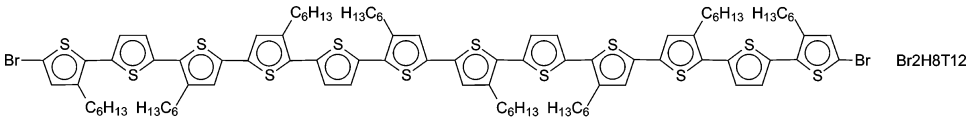

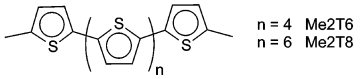

efficient (1%) solar cell.[8b] Finally, the properties of conjugated oligomers containing fluorene, fluorenone, and thiophene units have been recently reported.[9] These are models of the corresponding fluorene copolymers, and their structures are correlated with optical and electrochemical behavior.

The extension of conjugation with additional thiophene rings to the sexithiophene chain has also been investigated using an α,ω-dicarbaldehydeoctathiophene, an α,ω-dihexyldecathiophene, and an α,ω-dibromododecathiophene (see Chart 2). The influence, both steric and electronic, of such end substituents on the oligomer responses may be neglected due to the bulky hexyl substitution pattern and the length of the oligothiophene chain. For this reason the different end-capping substituents may change to some extent the redox potentials but will not influence significantly the conductive properties, thus allowing general conclusions to be drawn.

This paper describes a study complementary to that (part 1) previously reported for a long series of sexithiophene films.[5]

Experimental Section

Chemicals and Reagents. Acetonitrile was reagent grade (Uvasol, Merck) with a water content of <0.01%. The supporting

(6) (a) Larmat, F.; Reynolds, J. R.; Reinhardt, B. A.; Brott, L. L.; Clarson, S. J. *J. Polym. Sci., Part A* **1997**, *35*, 3627. (b) Tsuie, B.; Reddinger, J. L.; Sotzing, G. A.; Soloducho, J.; Katritzky, A. R.; Reynolds, J. R. *J. Mater. Chem.* **1999**, *9*, 2189. (c) Liu, B.; Yu, W.; Lai, Y.; Huang, W. *Macromolecules* **2000**, *33*, 8945. (d) Blondin, P.; Bouchard, J.; Beaupré, S.; Belletete, M.; Durocher, G.; Leclerc, M. *Macromolecules* **2000**, *33*, 5874. (e) Donat-Bouillud, A.; Levesque, I.; Tao, Y.; D'Iorio, M.; Beaupré, S.; Blondin, P.; Ranger, M.; Bouchard, J.; Leclerc, M. *Chem. Mater.* **2000**, *12*, 1931. (f) Charas, A.; Morgado, J.; Martinho, J. M. G.; Alcácer, L.; Cacialli, F. *Chem. Commun.* **2001**, 1216. (g) Pei, J.; Ni, J.; Zhou, X. H.; Cao, X. Y.; Lai, Y. H. *J. Org. Chem.* **2002**, *67*, 8104. (h) Asawapirom, Güntner, R.; Forster, M.; Farrell, T.; Scherf, U. *Synthesis* **2002**, 1136. (i) Pasini, M.; Destri, S.; Porzio, W.; Botta, C.; Giovanella, U. *J. Mater. Chem.* **2003**, *13*, 807. (j) Hou, Q.; Niu, Y.; Yang, W.; Yang, R.; Yuan, M.; Cao, Y. *Acta Polym. Sinica* **2003**, *2*, 161. (k) Charas, A.; Morgado, J.; Martinho, J. M. G.; Alcácer, L.; Lim, S. F.; Friend, R. H.; Cacialli, F. *Polymer* **2003**, *44*, 1843. (l) Vamvounis, G.; Schulz, G. L.; Holdcroft, S. *Macromolecules* **2004**, *37*, 8897. (m) Locklin, J.; Li, D.; Mannsfeld, S. C. B.; Borkent, E. J.; Meng, H.; Advincula, R.; Bao, Z. *Chem. Mater.* **2005**, *17*, 3366. (n) Lim, E.; Jung, B. J.; Lee, J.; Shim, H. K.; Lee, J.-I.; Yang, Y. S.; Do, L. M. *Macromolecules* **2005**, *38*, 4531. (o) Yang, L.; Ren, A. M.; Feng, J. K.; Wang, J. F. *J. Org. Chem.* **2005**, *70*, 3009. (p) Han, X.; Chen, X.; Vamvounis, G.; Holdcroft, S. *Macromolecules* **2005**, *38*, 1114. (q) Yang, R.; Tian, R.; Hou, Q.; Zhang, Y.; Li, Y.; Yang, W.; Zhang, C.; Cao, Y. *J. Polym. Sci., Part A* **2005**, *43*, 823.

(7) Meng, H.; Zheng, J.; Lovinger, A. J.; Wang, B. C.; Van Patten, P. G.; Bao, Z. *Chem. Mater.* **2003**, *15*, 1778.

(8) (a) Demadrille, R.; Rannou, P.; Bleuse, J.; Oddou, J. L.; Pron, A.; Zagorska, M. *Macromolecules* **2003**, *36*, 7045. (b) Demadrille, R.; Firon, M.; Leroy, J.; Rannou, P.; Pron, A. *Adv. Funct. Mater.* **2005**, *15*, 1547.

(9) Jaramillo-Isazaab, F.; Turner, M. L. *J. Mater. Chem.* **2006**, *16*, 83.

electrolyte tetrabutylammonium perchlorate (Bu_4NClO_4) and all other chemicals used for characterizations were reagent grade and used as received. All solvents (Aldrich) used for the chemical reactions were dried by standard procedures.

Butyllithium (BuLi), bromohexane, 2-isopropoxy-(4,4,5,5-tetramethyl)-1,3,2-dioxoborolane, *N*-bromosuccinimide (NBS), and tetrakis(triphenylphosphine)palladium ($(Ph_3P)_4Pd$) available from Aldrich or Acros were used as received, while bithiophene and 3-bromothiophene were purified by flash chromatography and distillation, respectively. Flash chromatography purifications were carried out using silica gel (200−300 mesh ASTM). Suzuki reactions with conventional heating were carried out under a nitrogen atmosphere.

3′-4′-Dihexyl-2,2′:5′,2″-terthiophene,[10] 5-bromo-3,3″-dihexyl-2,2′:5′,2″-terthiophene,[11] and 3,3‴,4⁗,3⁗′-tetrahexyl-2,2′:5′,2″:5″,2‴:5‴,2⁗:5⁗,2⁗′-sexithiophene[11] were prepared according to literature procedures.

The dimer of 3′-pentoxy-3,3″-dioctyl-2,2′:5′,2″-terthiophene (R6T6; see Chart 1)[12] and α,ω-dicarbaldehyde-3,3″,3⁗,3⁗′⁗′-tetrahexyloctathiophene (CA2H4T8; see Chart 2)[13] were prepared as in the literature. 5-(4,4,5,5-Tetramethyl-1,3,2-dioxoborolan-2-yl)-5′-hexyl-2,2′-bithiophene was synthesized as reported in ref 14.

5-(4,4,5,5-Tetramethyl-1,3,2-dioxaborolan-2-yl)-3′-4′-dihexyl-2,2′:5′,2″-terthiophene (1). To a solution of diisopropylamine (0.64 g, 6.42 mmol) in anhydrous THF (6 mL) was added dropwise butyllithium (3.9 mL, 6.42 mmol, in hexane) at −78 °C. The mixture was stirred at −78 °C for 20 min, warmed to 0 °C for 20 min, and cooled again at −78 °C. 3′-4′-Dihexyl-2,2′:5′,2″-terthiophene (296 mg, 0.72 mmol) was dissolved in anhydrous THF (1.5 mL), and 1.14 mL (0.68 mmol) of the just prepared lithium diisopropylamine (LDA) solution was added dropwise at −78 °C. A pink-orange mixture was formed and stirred at this temperature for 30 min, warmed to 0 °C for 10 min, and cooled again at −78 °C for 1 h. Then 0.6 mL of 2-isopropoxy-4,4,5,5-tetramethyl-1,3,2-dioxaborolane (0.46 g, 2.8 mmol) was added rapidly by a syringe, and the resulting solution was stirred at −78 °C for 1 h. During this period the color changed to orange. Then the bath was allowed to very slowly reach room temperature under stirring for 24 h. The desired terthiophene derivative (as confirmed by mass spectrometry and gas chromatography) obtained in a 70% yield was used directly for the next step, Suzuki coupling.

2-(3′,4′-Dihexyl-2,2′:5′,2″-terthiophene-5-yl)fluorenone (FOH2T3). To a Schlenk tube containing 0.57 mmol of a boronic derivative of terthiophene (**1**) in THF solution (4.5 mL) was added 1 mL of a 2 M solution of K_2CO_3, and the obtained mixture was stirred for 1 h. Separately a solution of 258 mg (0.57 mmol) of 2-bromofluorenone in 1.5 mL of anhydrous tetrahydrofuran (THF) was transferred via cannula to the flask containing the borolane derivative. After the addition of $(Ph_3P)_4Pd$ in catalytic amounts (15 mg), the reaction temperature was increased to 70 °C, and the reaction mixture was refluxed overnight under stirring, then quenched with acid water, and dried over magnesium sulfate. The solvent was removed, and the residue was purified by flash column chromatography (silica gel, hexane/dichloromethane = 8/2) to provide the title product as an orange solid (yield 97%). Mp: 130 °C. MS: *m*/*z* 595 ($M\bullet^+$). ^{1}H NMR (400 MHz, $CDCl_3$, δ, ppm): 7.90 (d, 1H, J = 1.5 Hz), 7.71 (dd, 1H, J = 1.5 Hz, J = 7.7 Hz), 7.68 (d, 1H, J = 7.7), 7.50−7.53 (br, 3H), 7.322−7.34 (br, 2H), 7.30 (dd, 1H, J = 3.6 Hz, J = 1.0 Hz) 7.15 (dd, 1H, J = 3.6 Hz, J = 1.0 Hz), 7.12 (d, 1H, J = 3.8 Hz), 7.07 (dd, 1H, J = 3.6, J = 5.4), 2.72 (m, 4H), 1.58 (br, 4H), 1.25−1.46 (br, 12H), 0.91 (m, 6H). UV−vis ($CHCl_3$): λ_{max} = 378 nm. FTIR (cast film on NaCl, cm^{-1}): 3094, 3066 (α and β C−H thiophene stretch), 2924 (C−H aliphatic stretch), 1717 (C═O stretch), 1601ν (C═C aromatic stretch), 1458ν (C═C thiophene stretch), 794 (C−H inner thiophene ring bending), 690 (C−H thiophene end-ring bending). Anal. Found: C, 73.95; H, 6.32; S, 16.27. Calcd for $C_{37}H_{38}OS_3$: C, 74.75; H, 6.4; S, 16.16.

2-(3′,4′-Dihexyl-2,2′:5′,2″-terthiophene-5-yl)fluorene (FH2T3). Following the same procedure described for oligomer FOH2T3**,** 157 mg (0.29 mmol) of **1**, 70.7 mg (0.29 mmol) of 2-bromofluorene, and 10 mg of $(Ph_3P)_4Pd$ gave an orange powder of oligomer FH2T3 in 87% yield. MS: *m*/*z* 581 ($M\bullet^+$). ^{1}H NMR (270 MHz, $CDCl_3$, δ, ppm): 7.78 (br, 3H), 7.65 (d, 1H, J = 8.17 Hz), 7.56 (d, 1H, J = 7.22 Hz), 7.42−7.32 (br, 4H), 7.14−7.06 (br, 3H), 3.95 (s, 2H), 2.72 (m, 4H), 1.58 (br, 4H), 1.25−1.46 (br, 12H), 0.91 (m, 6H). UV−vis (CH_2Cl_2): λ_{max} = 377 nm. FTIR (cast on NaCl, cm^{-1}): 3094, 3066 (α and β C−H thiophene stretch), 2924 (C−H aliphatic stretch), 1601 (C═C aromatic stretch), 1458 (C═C thiophene stretch), 794 (C−H inner thiophene ring bending, 690 (C−H thiophene end-ring bending). Anal. Found: C, 75.94; H, 6.92; S, 16.48. Calcd for $C_{37}H_{40}S_3$: C, 76.54; H, 6.89; S, 16.54.

5-Bromo-3,3″,4‴,3⁗′-tetrahexyl-2,2′:5′,2″:5″,2‴:5‴,2⁗:5⁗,2⁗′-sexithiophene (BrH4T6). To a solution of 3,3″,4‴,3⁗′-tetrahexyl-2,2′:5′,2″:5″,2‴:5‴,2⁗:5⁗,2⁗′-sexithiophene (213 mg, 0.25 mmol) in DMF (2 mL) was slowly added dropwise another solution of 101.4 mg (0.57 mmol) of NBS in 2 mL of the same solvent. The reaction was carried out over 40 h, keeping it in the dark, and then the mixture was poured onto ice and extracted with diethyl ether. After solvent evaporation a precipitate was formed which was removed by filtration. Separation by flash chromatography on silica gel using hexane as eluent yielded 48.5% of the titled monobromo derivative (>98% purity), 20% of the dibromo derivative, and 10% of the starting product. MS (EI): *m*/*z* 909 [M^+]. ^{1}H NMR (270 MHz, $CDCl_3$, δ, ppm): 7.17 (d, 1H, J = 5.19 Hz), 7.05 (br, 3H), 6.99 (br, 3H), 6.95 (d, 1H, J = 5.19 Hz), 6.92 (s, 1H), 2.75 (br, 8H), 1.65 (br, 8H), 1.38 (br, 8H), 1.31 (br, 16H), 0.88 (br, 12H). UV−vis ($CHCl_3$): λ_{max} = 413.6 nm. FTIR (cm^{-1}): 3067 (aromatic C−H stretch), 2924 (aliphatic C−H stretch), 1599 (C═C aromatic), 1465 (C═C thiophene), 794 (inner thiophene ring bending), 477 (C−Br stretching). Anal. Found: C, 63.24; H, 6.82; S, 21.00. Calcd for $C_{48}H_{61}S_6Br$: C, 63.31; H, 6.77; S, 21.13; Br, 8.80.

5,4″,3⁗′-Terhexyl-2,2′:5′,2″:5″,2‴:5‴,2⁗:5⁗,2⁗′-pentathiophene (H3T5). To a Schlenk tube were introduced 197 mg (0.52 mmol) of 5-(4,4,5,5-tetramethyl-1,3,2-dioxaborolan-2-yl)-5′-hexyl-2,2′-bithiophene, 216 mg (0.44 mmol) of 5-bromo-3,3″-dihexyl-2,2′:5′,2″-terthiophene, and 30 mg (0.026 mmol) of $(Ph_3P)_4Pd$. Then 4 mL of anhydrous THF and 2.5 mL of 2 M K_2CO_3 were added to this mixture under nitrogen. The reaction was refluxed under stirring overnight, thus producing an orange-brown precipitate which was extracted with dichloromethane (3 × 100 mL). The combined organic fractions were dried over anhydrous magnesium sulfate. Subsequently the solvent was removed by a rotary evaporator, giving an orange powder which was purified by flash chromatography (silica gel, hexane as eluent) to obtain an orange solid (234 mg, 82% yield). MS (EI): *m*/*z* 665 ($M\bullet^+$). ^{1}H NMR (400 MHz, $CDCl_3$, δ, ppm): 7.18 (br, 1H), 7.06−6.99 (br, 6H), 6.94 (d, 1H, J = 5.1 Hz), 6.68 (d, 1H, J = 3.45 Hz), 2.77 (m, 6H), 1.68 (m,

(10) Wang, C.; Benz, M. E.; Le Goff, E.; Schlinder, J. L.; Allbritton-Thomas, J.; Kannewurf, C. N.; Kanatzidis, M. G. *Chem. Mater.* **1994**, *6*, 401.
(11) Destri, S.; Ferro, D. R.; Khotina, I. A.; Porzio, W.; Farina, A. *Macromol. Chem. Phys.* **1998**, *1999*, 1973.
(12) Zotti, G.; Marin, R. A.; Gallazzi, M. C. *Chem. Mater.* **1997**, *9*, 2945.
(13) Olinga, T.; Destri, S.; Porzio, W. *Macromol. Chem. Phys.* **1997**, *198*, 1091.
(14) Josip, M. D.; Destri, S.; Pasini, M.; Porzio, W.; Pernstich, K. P.; Batlogg, B. *Synth. Met.* **2004**, *146*, 251.

6H), 1.40−1.31 (br, 18H), 0.91 (m, 9H). UV−vis ($CHCl_3$): λ_{max} = 407 nm. FTIR (cm^{-1}): 3067 (aromatic C−H stretch), 2924 (aliphatic C−H stretch), 1599 (C═C aromatic stretch), 1465 (C═C thiophene stretch), 794 (C−H inner thiophene ring bending), 690 (C−H thiophene end-ring bending). Anal. Found: C, 68.70; H, 7.25; S, 24.00. Calcd for $C_{38}H_{48}S_5$: C, 68.64; H, 7.23; S, 24.08.

Electrosynthesis of Sexithiophenes. Bulk sexithiophenes have been produced by exhaustive electrolysis (1.5−1.7 F mol^{-1}) at 0.7 V of 25 mg of FOH2T3 or FH2T3 in 25 mL of 1:1 (v/v) acetonitrile/CH_2Cl_2 + 0.1 M $NaClO_4$. The resulting green suspension of the oxidized products was reduced with a few drops of ammonia to a red-orange precipitate which was filtered off, washed with acetonitrile, and dried (yield 95% for both monomers).

Data for 5,5‴″-(Difluorenon-2-yl)-3′,4′,3‴″,4‴″-tetrahexyl-2,2′:5′,2″:5″,2‴:5‴,2⁗:5‴ ′,2⁗″-sexithiophene (FO2H4T6). ^{1}H NMR (270 MHz, $CDCl_3$, δ, ppm): 7.91 (d, 1H, J = 1.4 Hz), 7.71 (dd, 1H, J = 1.4 Hz, J = 7.9 Hz), 7.66 (m, 1H), 7.47−7.54 (br, 3H), 7.27−7.36 (br, 2H), 7.13−7.15 (br, 2H), 7.07 (d, 1H, J = 3.8 Hz), 2.74 (br, 4H), 1.13−1.72 (br, 16H), 0.88 (m, 6H). ^{13}C NMR ($CDCl_3$, δ, ppm): 148.69, 147.32, 145.75, 144.57, 143.89, 142.31, 142.21, 138.23, 137.97, 136.66, 136.54, 135.86, 132.91, 131.40, 130.73, 128.33, 128.06, 126.76, 126.03, 125.88, 125.61, 122.65, 122.57, 122.08, 121.71, 33.07, 32.10, 31.13, 29.87, 24.22, 15.75. FTIR (cast on NaCl, cm^{-1}): 3067 (C−H aromatic stretch), 2924 (C−H aliphatic stretch), 1718 (C═O), 1599 (C═C aromatic stretch), 1460 (C═C thiophene stretch), 779 (inner thiophene ring bending). MS (MALDI): m/z 1189 $[M + H]^+$. Anal. Found: C, 74.95; H, 6.32; S, 16.02. Calcd for $C_{74}H_{74}O_2S_6$: C, 74.84; H, 6.23; O, 2.69; S, 16.17.

Data for 5,5‴″-(Difluoren-2-yl)-3′,4′,3‴″,4‴″-tetrahexyl-2,2′:5′,2″:5″,2‴:5‴,2⁗:5⁗″,2‴″-sexithiophene (F2H4T6). ^{1}H NMR (270 MHz, *d*-TCE, δ, ppm): 7.80 (br, 3H), 7.67 (br, 1H), 7.58 (br, 1H), 7.40−7.35 (br, 3H), 7.17 (br, 2H), 7.09 (br, 1H), 3.96 (s, 2H), 2.76 (m, 4H), 1.62 (br, 4H), 1.25−1.46 (br, 12H), 0.91 (m, 6H). ^{13}C NMR (*d*-TCE, δ, ppm): 145.79, 145.71, 145.04, 142.84, 142.71, 142.17, 141.98, 138.14, 136.94, 134.19, 131.72, 131.04, 128.58, 128.28, 127.96, 126.76, 126.14, 125.58, 125.01, 123.77, 121.93, 121.58, 38.60, 33.07, 32.12, 31.28, 31.14, 29.89, 25.05, 24.23, 15.75. FTIR (cast on NaCl, cm^{-1}): 3066 (C−H aromatic stretch), 2924 (C−H aliphatic stretch), 1601 (C═C aromatic stretch), 1458 (C═C thiophene stretching), 794 (C−H inner thiophene ring bending). MS (MALDI): m/z 1161 $[M + H]^+$. Anal. Found: C, 76.76; H, 6.80; S, 16.40. Calcd for $C_{74}H_{78}S_6$: C, 76.65; H, 6.73; S, 16.56.

Electrosynthesis of Decathiophene and Dodecathiophene. Bulk decamer and dodecamer have been produced by exhaustive electrolysis (ca. 2.5 F mol^{-1}) at 0.8 V of 30 mg of H3T5 or BrH4T6 in 25 mL of CH_2Cl_2 + 0.1 M Bu_4NClO_4. The resulting dark suspension of the oxidized products was reduced with a few drops of hydrazine in 2 mL of acetonitrile to a red-orange solution (λ_{max}-($CHCl_3$) = 445 and 443 nm for H6T10 and Br2H8T12, respectively) which was evaporated, washed with acetonitrile (to remove supporting electrolyte, unreacted monomer, and side products), and dried (yield 97% and >90% for H6T10 and Br2H8T12, respectively).

Data for 5,5⁗″″″-Dibromo-3,3‴,4‴,3⁗″,4⁗″″,3″″″,4″″″″,3⁗″″″,4⁗″″″″-octahexyl-2,2′:5′,2″:5″,2‴:5‴,2⁗:5⁗″,2⁗″″:5⁗″″,2″″″:5″″″,2″″″″:5″″″″,2″″″″:5″″″″,2″″″″:5″″″″,2″″″″:5″″″″,2″″″″-dodecathiophene (Br2H8T12). H^1 NMR (400 MHz, $CDCl_3$, d, ppm): 7.08 (s, 2H), 7.05 (d, 1H, J = 3.78 Hz), 6.99 (m, 4H), 6.89 (s, 1H), 2.75 (br, 8H), 1.67 (br, 8H), 1.39 (br, 8H), 1.33 (br, 16H), 0.88 (br, 12H). ^{13}C NMR ($CDCl_3$, d, ppm): 139.68, 139.56, 139.45, 135.40, 134.90, 134.81, 134.14, 134.00, 133.87, 133.74, 131.72, 130.90, 128.64, 128.59, 128.32, 125.60, 125.58, 125.00, 124.90, 30.69, 30.65, 29.56, 29.49, 28.68, 28.59, 28.26, 28.12, 21.61, 13.03. FTIR (cm^{-1}): 3067 (aromatic C−H stretch), 2924 (aliphatic C−H stretch), 1465 (C═C thiophene stretch), 794 (inner thiophene ring bending), 477 (C−Br stretch). MS (MALDI): m/z 1816 (M^+). Anal. Found: C, 63.21; H, 6.88; S, 20.70. Calcd for $C_{96}H_{120}S_{12}Br_2$: C, 63.44; H, 6.61; S, 21.15.

Data for 5,5⁗″″″″,4″,3‴″,4⁗″″,3⁗″″″-Hexahexyl-2,2′:5′,2″:5″,2‴:5‴,2⁗:5‴,2″″:5⁗″,2⁗″″:5″″″,2″″″:5″″″,2″″″″:5″″″″,2″″″″:5″″″″,2″″″″-decathiophene (H6T10). ^{1}H NMR (400 MHz, $CDCl_3$, δ, ppm): 7.07 (s, 2H), 7.03 (d, 1H, J = 3.75 Hz), 7.02−6.97 (m, 4H), 6.67 (d, 1H, J = 3.52 Hz), 2.77 (m, 6H), 1.66 (m, 6H), 1.39 (m, 6H), 1.32 (m,-12H), 0.89 (m, 9H). ^{13}C NMR ($CDCl_3$, δ, ppm): 144.74, 139.57, 139.54, 136.00, 135.82, 134.86, 134.32, 134.15, 133.99, 133.53, 128.58, 128.42, 125.63, 125.47, 125.00, 124.97, 123.84, 123.20, 122.62, 122.44, 30.69, 30.56, 30.50, 29.50, 29.21, 28.59, 28.27, 27.75, 21.61, 21.55, 13.04. FTIR (cm^{-1}): 3067 (aromatic C−H stretch), 2924 (aliphatic C−H stretch), 1465 (C═C thiophene stretch), 794 (inner thiophene ring bending). MS (MALDI): m/z: 1328. Anal. Found: C, 68.88; H, 7.12; S, 23.95. Calcd for $C_{76}H_{94}S_{10}$: C, 68.76; H, 7.08; S, 24.11.

Apparatuses and Procedures. Experiments were performed at room temperature under nitrogen in three-electrode cells. The counter electrode was platinum; the reference electrode was silver/0.1 M silver perchlorate in acetonitrile (0.34 V vs SCE). The voltammetric apparatus (AMEL, Italy) included a 551 potentiostat modulated by a 568 programmable function generator and coupled to a 731 digital integrator.

Oligothiophenes were investigated as films cast from $CHCl_3$ solutions, with the exception of FO2H4T6 and F2H4T6, which were usually electrodeposited from the corresponding terthiophene. Their electrochemistry was performed in acetonitrile + 0.1 M Bu_4NClO_4.

The working electrode for cyclic voltammetry was a platinum minidisk electrode (0.003 cm^2). For electronic spectroscopy a 0.8 × 2.5 cm indium−tin oxide (ITO) sheet (ca. 20 Ω/square resistance, from Balzers, Liechtenstein) was used.

^{1}H and ^{13} C NMR (270 and 400 MHz) spectra were measured with a Bruker Avance instrument. Gas chromatograms were obtained using an Agilent Network GC System 6890N instrument. FTIR spectra were recorded either on a Bruker IFS 48 instrument or on a Perkin-Elmer 2000 FTIR spectrometer, using KBr pellets unless otherwise specified. FTIR spectra of films were taken in reflection−absorption mode. Electronic spectra were obtained on either a Perkin-Elmer Lambda 15 or a Lambda 900 Perkin-Elmer spectrometer. Electron-impact mass spectrometry measurements were performed on a VG ZAB-2F spectrometer equipped with an FI/FD ion source kept at ca. 200 °C operating at 8 kV accelerating and 4 kV output potentials and with the emitter activated according to the standard VG micromass procedure. Matrix-assisted laser desorption ionization (MALDI) mass spectra were obtained on an Ultraflex II mass spectrometer (Bruker Daltonics) operating both in the positive reflectron and in the linear modes, using 2,5-dihydroxybenzoic acid as the matrix.

Electrochemical quartz crystal microbalance (EQCM) analyses were performed with a platinum-coated AT-cut quartz electrode (0.2 cm^2), resonating at 9 MHz, onto which the polymers were deposited. The oscillator circuit was homemade, and the frequency counter was Agilent mod.53131A. Data were collected by a microcomputer with homemade analyzing software. The dry mass and charge measurements were performed according to the procedure previously published.[15]

(15) Zotti, G.; Zecchin, S.; Schiavon, G.; Groenendaal, L. *Chem. Mater.* **2000**, *12*, 2996.

Table 1. Terthiophene Oxidation CV Peak Potentials (E_p) and Absorption Maxima (λ)

terthiophene	E_p/V	λ^a/nm
FOH2T3	0.73	376
FH2T3	0.60	377
MeT3[31]	0.70	360

[a] In $CHCl_3$.

ESR spectra were taken on a Bruker ER 100D following the procedure previously described.[16] Absolute spin calibration was performed with VOSO4.5H2O crystals and *g* value calibration with thin films of DPPH ($g = 2.0036$[17]).

The apparatus and procedures used for the in situ conductivity experiments were previously described in detail.[18,19] The electrode for conductivity measurements was typically a two-band platinum electrode (0.3 cm × 0.01 cm for each band) with an interband spacing of 20 μm. In the case of conductivities lower than 10^{-2} S cm^{-1}, the electrode was a microband array platinum electrode (5 μm bandwidth, 100 nm thickness) with an interband spacing of 5 μm. The deposit was thick enough to ensure minimum resistance, under which condition the conductivity σ is given by $\sigma = k/(R - R_0)$, where R is the measured resistance, R_0 the lead resistance, and k the cell constant.

Results and Discussion

Electrochemical Synthesis of End-Capped Sexithiophenes. The oxidation potential of 3,4-dialkylterthiophene is 0.62 V,[20] that of fluorene is 1.35 V,[21] and that of fluorenone is 1.70 V.[22] From these values it is clear that oxidation of FOH2T3 and FH2T3 is localized at the terthiophene moiety. The radical cation produced in this way couples (dimerizes) at the free α-position, giving the fully conjugated sexithiophene.

The terthiophenes were investigated in acetonitrile/CH_2Cl_2 (1:1) mixture + 0.1 M Bu_4NClO_4 because chlorinated solvent addition imparts an appreciable solubility to the monomer.

The cyclic voltammogram shows an irreversible oxidation process at oxidation peak potentials given in Table 1, the irreversibility of which is due to coupling to the dimer.[23] The electrochemical process is very fast, becoming a one-electron reversible one only at scan rates higher than 20−50 V s^{-1} (Figure 1a). Kinetic analysis according to a second-order dimerization process[24] has given FOH2T3 a rate constant of ca. 10^5 M^{-1} s^{-1}, comparable with that of MeT3[25] and therefore confirming the nonparticipation of the fluorenonyl substituent.

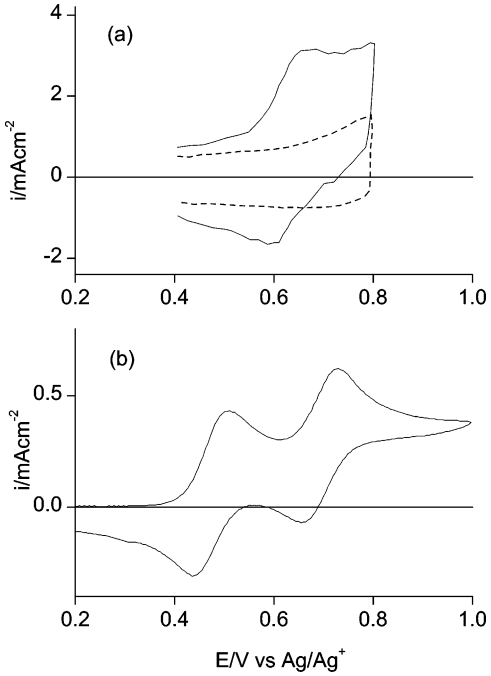

Figure 1. Cyclic voltammograms of (a) FOH2T3 (5×10^{-4} M) in acetonitrile/CH_2Cl_2 + 0.1 M Bu_4NClO_4 and (b) H3T5 (10^{-3} M) in CH_2Cl_2 + 0.1 M Bu_4NClO_4. Scan rate (a) 50 V s^{-1} and (b) 0.1 V s^{-1}.

The oxidation peak potentials are related to the electron donor or acceptor properties of the substituents, so fluorenone shifts the potential anodically by 0.13 V compared to fluorene.

The cyclic voltammogram of FOH2T3 also shows a reversible one-electron reduction process at $E^0 = -1.47$ V due to the carbonyl moiety.

Oxidation results in an efficient α-dimerization. Repetitive CV up to the oxidation peak potential displays the progressive deposition of the product of coupling, namely, the sexithiophene. Bulk sexithiophenes were produced potentiostatically as detailed in the Experimental Section.

The sexithiophenes are soluble in $CHCl_3$. Their formulas were confirmed by several techniques such as MALDI, NMR, and FTIR. MALDI shows a single peak at *m*/*z* corresponding to the $[M + H]^+$ ion. Proton and carbon NMR spectra of both FO2H4T6 and F2H4T6 agree with dimer formation. The dd signals at 7.07 and 7.15 ppm typical of the end thiophene ring present in the proton spectrum of FO2H4T6 are not evident, and the signal at 7.30 ppm attributable to the α-proton of the same ring disappears. Quite similar observations are applicable to the F2H4T6 spectrum. Each FTIR spectrum practically superimposes on that of the corresponding monomer with the exception of the band at 690 cm^{-1}, due to the out-of-plane bending modes of the hydrogen atoms at the terminal thiophene rings, which disappears while a single strong band at 790 cm^{-1}, due to the corresponding mode of the inner thiophene rings, becomes more evident.[26]

Redox potentials (see below) and UV−vis absorption maxima of the sexithiophene films are summarized in Table 2.

(16) Zotti, G.; Schiavon, G. *Synth. Met.* **1989**, *31*, 347.
(17) Inzelt, G.; Day, R. W.; Kinstle, J. F.; Chambers, J. Q. *J. Phys. Chem.* **1983**, *87*, 4592.
(18) Schiavon, G.; Sitran, S.; Zotti, G. *Synth. Met.* **1989**, *32*, 209.
(19) Aubert, P. H.; Groenendaal, L.; Louwet, F.; Lutsen, L.; Vanderzande, D.; Zotti, G. *Synth. Met.* **2002**, *126*, 193.
(20) Dini, D.; Decker, F.; Zotti, G. *Electrochem. Solid State Lett.* **1998**, *1*, 217.
(21) Hapiot, P.; Lagrost, C.; Le Floch, F.; Raoult, E.; Rault-Berthelot, J. *Chem. Mater.* **2005**, *17*, 2003.
(22) Zecchin, S.; Schiavon, G.; Tomat, R.; Zotti, G. *J. Electroanal. Chem.* **1986**, *215*, 377.
(23) Demanze, F.; Godillot, P.; Garnier, F.; Hapiot, P. *J. Electroanal. Chem.* **1996**, *414*, 61.
(24) Andrieux, C. P.; Audebert, P.; Hapiot, P.; Saveant, J. M. *J. Phys. Chem.* **1991**, *95*, 10158.
(25) Zotti, G.; Schiavon, G.; Berlin, A.; Pagani, G. *Chem. Mater.* **1993**, *5*, 430.
(26) Akimoto, M.; Furukawa, Y.; Takeuchi, Y.; Harada, I. *Synth. Met.* **1986**, *15*, 353.

Table 2. Oligothiophene Film Oxidation Redox Potentials ($E°$), Adsorption Maxima (λ), and Maximum Conductivities (σ)

oligothiophene	$E°$/V	λ^a/nm	σ/(S cm^{-1})
FO2H4T6	0.22, 0.52, 0.9	428	−, 0.005, 0.1
F2H4T6	0.26, 0.37, 0.7	428	−, 0.004, 0.07
Me2T6[31,40]	0.50, 0.72	445[b]	−, 0.01
CA2H4T8	0.40, 0.75	462	0.0003, 0.003
Me2T8[31,40]	0.50	−	0.002, 0.02
H6T10	0.23	445	0.03
Br2H8T12	0.20	443	3.0

[a] In $CHCl_3$. [b] In chlorobenzene.

Electrochemical Synthesis of End-Capped Decathiophene and Dodecathiophene. The α,ω-capped decathiophene H6T10 and dodecathiophene Br2H8T12 were prepared by anodic coupling of the α-capped quinquethiophene H3T5 (λ_{max} = 408 nm in $CHCl_3$) and sexithiophene BrH4T6 (λ_{max} = 414 nm in $CHCl_3$) similarly to the reported electrochemical dimerization of didecylsexithiophene.[27]

In fact, the cyclic voltammograms of H3T5 and BrH4T6 in CH_2Cl_2 + 0.1 M Bu_4NClO_4 at a low scan rate (Figure 1b) show two one-electron reversible oxidation processes at $E°$ = 0.47 and 0.69 V (H6T10) and 0.47 and 0.63 V (Br2H8T12). In any case the one-electron-oxidized species (radical cation) is not stable in the long run, undergoing dimerization on the time scale of electrolysis. Thus, electrolytic oxidation produces the α,ω-capped decathiophene, even if the oxidation is performed at potentials corresponding to dication formation, since redox exchange between the dication and neutral species is very fast. The dimers, which are produced in the fully oxidized state, can be reduced with hydrazine to the undoped state (λ_{max} = 445 and 443 nm in $CHCl_3$ for H6T10 and Br2H8T12, respectively).

The oligothiophenes are soluble in $CHCl_3$. Their formulas were confirmed by MALDI and NMR. The proton NMR spectra of the oligomers show, in the aromatic region, four signals corresponding to eight protons present in half a molecule because four signals overlap in a broad multiplet. Redox potentials and UV−vis absorption maxima of the films (see below) are summarized in Table 2.

Electrochemistry of End-Capped Sexithiophene Films. *Cyclic Voltammetry*. The oxidation cyclic voltammograms of FO2H4T6 and F2H4T6 deposits, driven up to 0.8 and 0.6 V, respectively, are shown in Figure 2a,b. The first clearly shows two oxidation and two backward reduction peaks, whereas the second displays a single oxidation and two backward reduction peaks.

The electron stoichiometry for the overall redox process was determined by spectrophotometry, dissolving deposits of known charge content in chlorobenzene and comparing the absorption at the maximum with that of a standard sample. The result is that the overall redox cycle involves 2 F mol^{-1}.

The determination of the electron stoichiometry was also made directly on the film with EQCM analysis. Thus, deposits give a ratio of reversible charge to dry weight (at the undoped state) which confirms the passage of 2 F mol^{-1}.

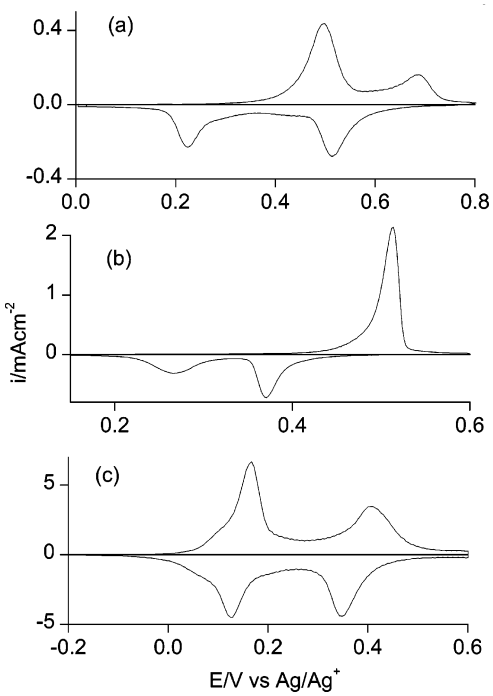

Figure 2. Cyclic voltammograms of (a) FO2H4T6, (b) F2H4T6, and (c) R6T6 films in acetonitrile + 0.1 M Bu_4NClO_4. Scan rate 0.1 V s^{-1}.

The oxidation is a slow electron transfer between adjacent oligothiophene chains, whereas in the backward reduction the process is fast. Therefore, the peak potentials in reduction have been taken as a more precise evaluation of the redox potentials[28] (Table 2).

Two electrons, removed in a single process from F2H4T6 and in two steps from FO2H4T6, are given back in two isoelectronic (one-electron) processes. The potential separation between the redox processes of F2H4T6 is only 0.1 V vs 0.3 V in FO2H4T6, which is due to a negative shift of the second redox potential in the former compound compared with FO2H4T6 caused by the presence of the more electron donor fluorene terminal groups[29] and accounts for the absence of splitting of the forward two-electron oxidation peak.

Chromatic changes accompany the oxidation of the sexithiophenes as well illustrated by FO2H4T6 (Figure 3). The undoped film (maximum absorption at 460 nm) after one-electron oxidation shows a broad polaron maximum at ca. 700 cm^{-1} and at the full two-electron (bipolaron) state shows the relevant well-known broad absorption extending into the NIR region.[30]

After the two-electron oxidation process a further flat oxidative process with capacitive properties follows starting from ca. 0.9 and 0.7 V for FO2H4T6 and FO2F2H4T6, respectively (Figure 4). Stability problems limit the exploitable range to 1.2−1.3 V, where the charge measured for the last oxidation process corresponds (by EQCM analysis) to ca. 0.8 (FO2H4T6) and 1.5 (F2H4T6) F mol^{-1}. The increased stoichiometry of the latter compared with FO2H4T6 is due to the lower oxidation potential produced by the more

(27) Delabouglise, D.; Hmyene, M.; Horowitz, G.; Yassar, A.; Garnier, F. *Adv. Mater.* **1992**, *4*, 107.
(28) Xu, Z. G.; Horowitz, G. *J. Electroanal. Chem.* **1992**, *335*, 123.
(29) Hapiot, P.; Kispert, L. D.; Konovalov, V. V.; Saveant, J. M. *J. Am. Chem. Soc.* **2001**, *123*, 6669.
(30) Fichou, D.; Horowitz, G.; Xu, B.; Garnier, F. *Synth. Met.* **1990**, *39*, 243.

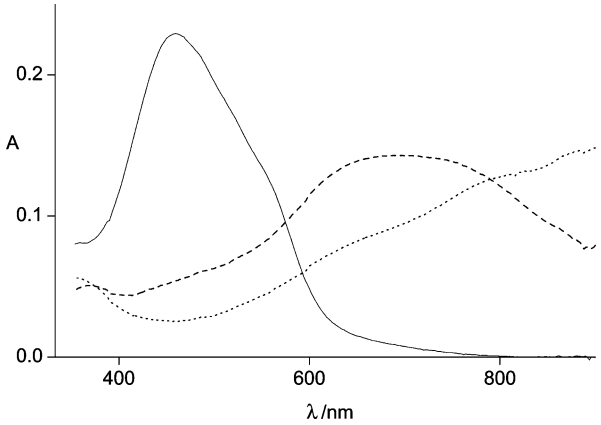

Figure 3. Spectroelectrochemistry of the FO2H4T6 film in acetonitrile + 0.1 M Bu_4NClO_4: (—) undoped, (---) polaron, and (···) bipolaron state.

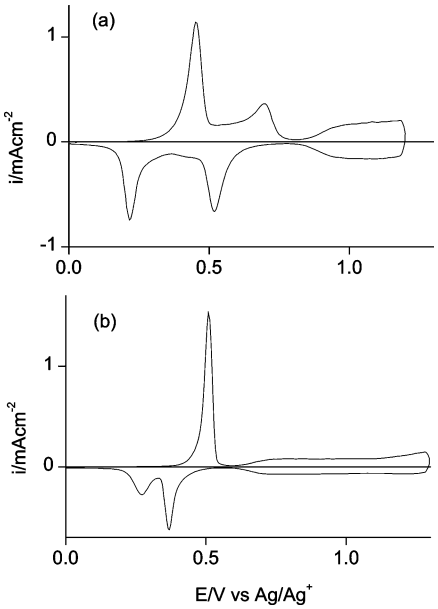

Figure 4. Extended cyclic voltammograms of (a) FO2H4T6 and (b) F2H4T6 films in acetonitrile + 0.1 M Bu_4NClO_4. Scan rate 0.1 V s^{-1}.

electron rich fluorene moieties. Thus, the more anodic feature appears to correspond to a distinct further multielectron redox process.

The reduction process of FO2H4T6 ($E° = -1.70$) is only partially reversible mainly due to dissolution of the produced radical anions and involves the same charge of the two-electron oxidation process. Since reduction involves one electron per fluorenone moiety, the result corresponds to the expected reduction of both fluorenone ends.

Location of Stored Positive Charge. As for the terthiophene moiety, the sexithiophene core is more easily oxidized than the fluorene or fluorenone ends, so the initial two-electron oxidative charge will be strongly localized on the oligothiophene core of the linear molecule.

Among the reported oxidations of sexithiophenes, it is worth mentioning the methyl-capped Me2T6[31] and didodecyl-capped D2T6,[32] which are oxidized in two one-electron processes at 0.50 and 0.72 V (Me2T6) and at 0.39 and 0.77 V (D2T6) vs Ag/Ag^+.

In neither case were oxidation processes beyond the dication observed. Instead, a series of regular head-to-tail-coupled oligo(3-hexylthiophene)s in solution[33] have revealed for the hexamer the oxidation of the oligothiophene chain up to the radical trication in three reversible one-electron steps at $E° = 0.35$, 0.50, and 1.25 V vs Ag/Ag^+. Thus, the existence of a stable trication state is made possible by full alkyl substitution.

Following these results, we should expect in our case approximate values of 0.4 and 0.7 V for the first two oxidation processes of the sexithiophene core. Instead, we have values considerably lower and depending on whether fluorene or fluorenone is the substituent. This is a first indication that the substituent participates in the oxidation processes. Furthermore, for the third oxidation process we measure $E°$ values of 0.7 V with fluorene and 0.9 V with fluorenone; i.e., a strong influence of the substituent is evident. Such values are much lower than the values for the isolated substituent moieties (1.35 V for fluorene and 1.70 V for fluorenone).

All these data support the idea that the core and end moieties share their conjugated π-electron systems. In particular, it is very likely that in the two-electron-oxidized state a low-lying energy band, available for further oxidation and (as we will see later) for enhanced conduction, is delocalized over the whole conjugated chain.

CV Hysteresis and Capacity. The cyclic voltammogram of sexithiophene films shows for FO2H4T6 (Figure 2a) two oxidation and two backward reduction peaks with hysteresis, i.e., with an unusually high separation between forward and backward peak potentials. Moreover, a current plateau appears between reduction peaks (capacitive current).

The asymmetry of reversibility is better evidenced from the relationship of charge vs potential showing that the two-electron oxidative charge is recovered in two 1:1 steps but is given in two 3:1 steps. This hysteretic behavior is not scan rate dependent. As shown in Figure 5a the CV current increases linearly with scan rate without any change in the peak potential values. This fact suggests that the process is not controlled by electron transfer but by structural (e.g., solvation) phenomena.

In agreement with this the cyclic voltammogram of films of R6T6, a noncapped sexithiophene made stable toward oxidative coupling by its substitution pattern,[12] shows two one-electron reversible processes (Figure 2c) noticeably symmetric, i.e., without marked hysteretic features. Movement of the electrolyte within the material is in this case favored by solvent affinity with the alkoxy substituents.

EQCM analysis of the oxidation process of FO2H4T6 supports this point of view further. The analysis shows a huge mass increase with oxidation. The relationship of mass and charge is linear with slope $F\Delta m/Q$ = ca. 530 g mol^{-1} for the two-electron process and 100 g mol^{-1} for the following process. The former corresponds to the assumption

(31) Zotti, G.; Schiavon, G.; Berlin, A.; Pagani, G. *Chem. Mater.* **1993**, *5*, 620.
(32) Bauerle, P.; Segelbacher, U.; Gaudl, K. U.; Huttenlocker, D.; Mehring, M. *Angew. Chem., Int. Ed. Engl.* **1993**, *32*, 76.
(33) (a) Kirschbaum, T.; Azumi, R.; Mena-Osteritz, E.; Bäuerle, P. *New J. Chem.* **1999**, *23*, 241. (b) Cremer, J.; Mena-Osteritz, E.; Pschierer, N. G.; Müllen, K.; Bäuerle, P. *Org. Biomol. Chem.* **2005**, *3*, 985.

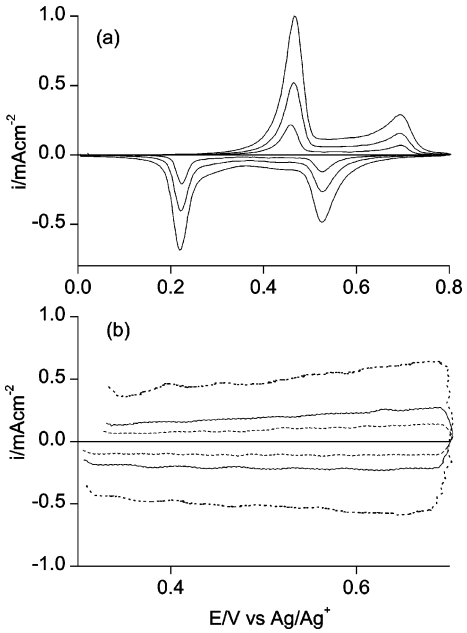

Figure 5. Cyclic voltammograms of the FO2H4T6 film in acetonitrile + 0.1 M Bu_4NClO_4 (a) in the 0.0−0.8 V range and (b) in the 0.4−0.7 V range. Scan rates (a) 0.02, 0.05, and 0.1 V s^{-1} and (b) 0.1, 0.2, and 0.5 V s^{-1}.

of perchlorate anion plus a big amount of solvent (ca. 10 acetonitrile molecules per electron), whereas the second corresponds to the assumption of the perchlorate anion solely. Since the undoped material is insoluble, no effective solvation is operating in the undoped state.

Hysteresis in fact reflects strong attractive interactions among the molecules in the crystals[34] opposing counterion and solvent ingress into the structure. This effect is normally observed when solid−solid electrochemical transformations are accompanied by large crystalline changes.[35]

A similar reasoning may be made for F2H4T6 though a single CV oxidation peak is shown. In fact, thiophene oligomers such as sexithiophene itself[31] and tetradecyl-substituted dodecathiophene[36] show a single oxidation and two reduction peaks in CV.

The capacitive behavior of FO2H4T6 is clearly shown if CV is performed between 0.3 and 0.7 V (Figure 5b), i.e., in the potential domain of the polaron−bipolaron state. It may be noted that the cyclic voltammogram for scans following the first one is just a capacitive plateau with current linearly linked to the scan rate. A similar feature can be observed in the case of Me2T6 films[31] and appears to be correlated with a strong crystal packing of the sexithiophene molecules.

The capacitive properties, which are attributable to the availability of electron-filled states of constant density, are displayed at the early states of oxidation, i.e., already at levels lower than the one-electron oxidation state.

In conclusion, both the hysteretic and the capacitive properties of the investigated sexithiophene films are due to a close packing of the oligomer chains, in particular with the fluorenone ends. As confirmation it has been shown that

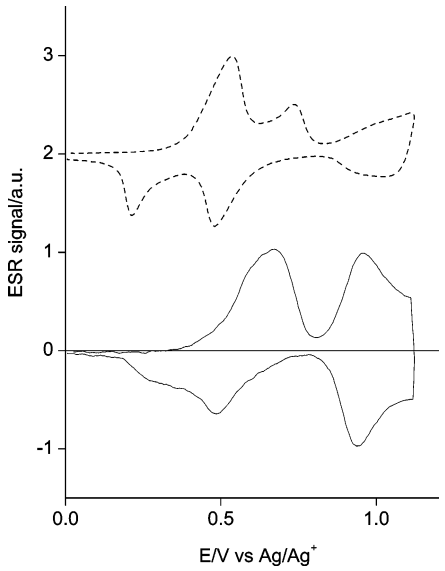

Figure 6. In situ ESR signal vs potential of the FO2H4T6 film in acetonitrile + 0.1 M Bu_4NClO_4 (the signal is inverted in the backward scan for clarity). Scan rate 0.02 V s^{-1}. The dashed line shows the cyclic voltammogram for comparison.

Table 3. Oligothiophene ESR *g* Values and One-Electron Spin Concentrations N_s

oligothiophene	*g*	N_s/(spin mol^{-1})	oligothiophene	*g*	N_s/(spin mol^{-1})
FO2H4T6	2.0023, 2.0030	0.10	CA2H4T8	2.0023	0.20
F2H4T6	2.0023, 2.0030	0.10	H6T10	2.0025	0.08
Me2T6[31]	2.0025	0.04	Br2H8T12	2.0028	0.07

the fluorenone moiety is capable to pack strictly thanks to strong interactions among adjacent molecules.[37]

In Situ ESR of End-Capped Sexithiophene Films. Oxidation of the sexithiophene films produces an ESR signal (1.5−3 G wide) which attains a maximum before the second oxidation peak potential and decreases almost to zero at two-electron oxidation (Figure 6). This may be explained with the subsequent formation of the paramagnetic radical cation (polaron) and of the diamagnetic dication (bipolaron).[31] On the reverse scan the signal reappears with peaks in correspondence with the cyclic voltammetric peaks and a more or less defined plateau in the intermediate potential range. The low value of spin concentration for the one-electron-oxidized oligomer (see Table 3) must be due to spin pairing in π-dimers.[38]

Oxidation at the higher potential redox cycle, where the dication is converted to a trication, produces once more an ESR signal (Figure 6). The values of $g = 2.0023$ (cation) and 2.0030 (trication) indicate a different location of the unpaired electron at the different redox states, i.e., at the carbon polyene backbone (cation) and at an orbital with participation of the thiophene sulfur atoms (trication).

Maximum spin concentration was evaluated at the reverse reduction scan, where we may assume that equilibrium conditions are attained.[28] The spin concentration at the one-electron and three-electron oxidation states is ca. 0.1 spin mol^{-1} for both sexithiophenes.

(34) Laviron, E. *J. Electroanal. Chem.* **1981**, *122*, 37.
(35) Neufeld, A. K.; Madsen, I.; Bond, A. M.; Hogan, C. F. *Chem. Mater.* **2003**, *15*, 3573.
(36) Yassar, A.; Delabouglise, D.; Hmyene, M.; Nessak, B.; Horowitz, G.; Garnier, F. *Adv. Mater.* **1992**, *4*, 490.
(37) Baldwin, S. L.; Baughman, R. G. *Acta Crystallogr., C* **1993**, *49*, 1840.
(38) Miller, L. L.; Mann, K. R. *Acc. Chem. Res.* **1996**, *29*, 417 and references therein.

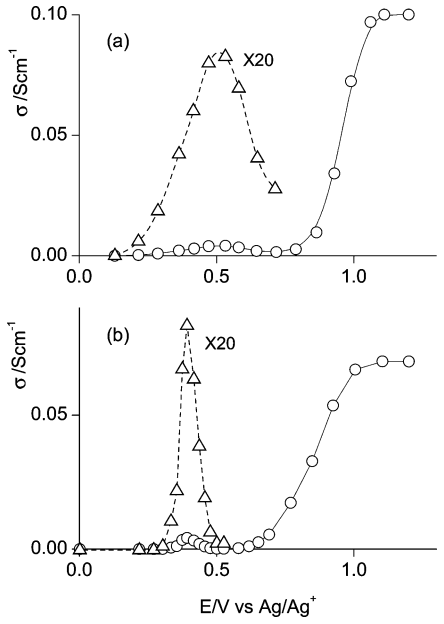

Figure 7. In situ conductivity vs potential of (a) FO2H4T6 and (b) F2H4T6 films in acetonitrile + 0.1 M Bu_4NClO_4.

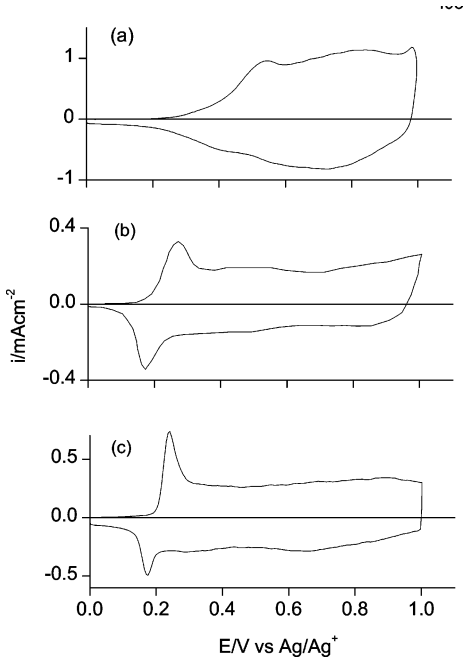

Figure 8. Cyclic voltammograms of (a) CA2H4T8, (b) H6T10, and (c) Br2H8T12 films in acetonitrile + 0.1 M Bu_4NClO_4. Scan rate 0.1 V s^{-1}.

In Situ Conductivity of End-Capped Sexithiophene Films. For this type of analysis, FO2H4T6 films were electrodeposited whereas F2H4T6 were better cast from a chloroform solution of the bulk material prepared as in the Experimental Section. Since the behaviors of samples produced in either way are the same, we may state that the role of morphology (if different) in determining the conductivity of our samples is minor.

The in situ conductivity has been measured as a function of the potential going from the oxidized to the undoped state of the materials (Figure 7). Equilibrium conditions are in this way continuously maintained as ascertained previously for polythiophene.[16]

FO2H4T6 is low-conducting both in the undoped and in the two-electron-oxidized state through a conducting state with a maximum conductivity of 5×10^{-3} S cm^{-1}. The maximum is displayed at the potential of the cation/dication transition, indicating mixed-valence conduction.[3] A similar response with a maximum conductivity of 1×10^{-2} S cm^{-1} was previously obtained for Me2T6.[40] Also a neutral−polaron conduction is normally observed in sexithiophenes,[5] but in this case it is not discernible from the closely following and much higher polaron−bipolaron conductivity. The conductive response of FO2H4T6 is broader than that of F2H4T6, which may be accounted for by the wider potential range of the stability of the former polaron state.

At charges higher than two electrons a sigmoid conductive state, with a plateau value of ca. 10^{-1} S cm^{-1}, is developed as for the setting-in of a metal-like conduction. The same behavior has been observed for F2H4T6 (Figure 7b).

Conductivity maxima of the oligothiophenes are summarized in Table 2.

End-Capped Octathiophene, Decathiophene, and Dodecathiophene. *Electrochemistry*. CA2H4T8 as a film cast from $CHCl_3$ solution shows its reversible oxidation as a couple of processes with a capacitive feature at the anodic side (Figure 8a). H6T10 and Br2H8T12 show a single reversible oxidation process followed by a capacitive plateau (Figure 8b,c). Stability problems limit the exploitable range to 1.0 V for all the oligothiophenes.

It is worth noting that Br2H8T12 represents the longest regular oligothiophene ever investigated electrochemically in the solid state.

EQCM Analysis. The electron stoichiometry was obtained by EQCM analysis. The CA2H4T8 deposits give a ratio of reversible charge to dry weight (at the undoped state) which corresponds to the passage of 2 F mol^{-1} (at 1.0 V switching potential). In any case the open capacitive response at the anodic limit allows in principle more charge to be retrieved from the same electron band at higher potentials. For the H6T10 deposits the ratio of reversible charge to dry weight (at the undoped state) indicates the passage of 2.0 F mol^{-1} at a switching potential of 0.7 V and 2.3 F mol^{-1} at 1.0 V; i.e., only a moderate increase of stored charge is observed. In marked contrast Br2H8T12, with a similar redox potential, has shown the passage of 3.5 F mol^{-1} (at 1.0 V switching potential), i.e., a much higher amount of doping charge.

ESR. As in the case of the sexithiophenes, oxidation of these oligothophene films produces an ESR signal which goes through a maximum and decreases to zero at two-electron oxidation. The maximum spin concentration (0.2 spin mol^{-1} for the octamer and 0.07−0.08 spin mol^{-1} for deca- and dodecathiophene) is recorded at a low redox charge, corresponding to ca. 0.5 F mol^{-1}. This indicates that the polaron is unstable, the oxidation going to the bipolaron almost at the same potential, particularly for the deca- and dodecathiophene. In fact, the two subsequent one-electron oxidation processes of oligothiophenes are progressively closer as the oligomer length increases.[41]

(39) Chidsey, C. D.; Murray, R. W. *J. Phys. Chem.* **1986**, *90*, 1479.
(40) Zotti, G.; Schiavon, G.; Berlin, A.; Pagani, G. *Adv. Mater.* **1993**, *5*, 551.

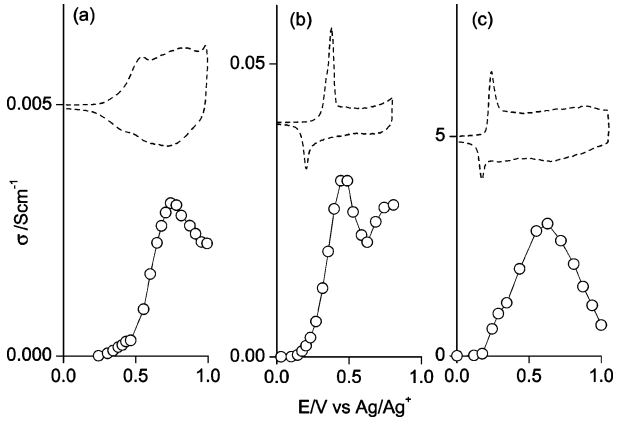

Figure 9. In situ conductivity vs potential of (a) CA2H4T8, (b) H6T10, and (c) Br2H8T12 films in acetonitrile + 0.1 M Bu_4NClO_4. The dashed lines show the cyclic voltammograms for comparison.

Conductivity. The in situ conductivity of the CA2H4T8 film as a function of the potential (Figure 9a) goes through a conducting state with two maxima of conductivity. The maxima are displayed at the potentials of the neutral/cation (3×10^{-4} S cm^{-1}) and cation/dication (3×10^{-3} S cm^{-1}) transitions. After the second maximum, where capacitive properties are kept, the conductivity keeps a high value.

Reexamining the results previously obtained with Me2T8,[40] the picture of this octamer appears to be the same apart from the ca. 10 times higher values of conductivity (0.002 and 0.02 S cm^{-1}) in Me2T8, which are accounted for by the absence of the steric hindrance to electron hopping introduced by hexyl substituents.

The in situ conductivity of the H6T10 film (Figure 9b) goes through a maximum (0.03 S cm^{-1}) at 0.5 V (with no redox conductivity at the redox potential $E^\circ = 0.23$ V), then decreases moderately, and then increases at higher potentials, attaining a plateau (0.025 S cm^{-1}). The plot of conductivity vs charge (Figure 10b) shows a moderate contribution of redox conductivity at the polaron−bipolaron mixed valence (1.5 F mol^{-1}) over a substantially metal-like conductive plateau.

The in situ conductivity of the Br2H8T12 film as a function of potential (Figure 9c) goes through a maximum (3.0 S cm^{-1}) and then decreases. As a function of doping charge (Figure 10c), the conductivity, after an initial low-conducting start (up to ca. 15% of the total reversible charge), due to polarons and dimerized polarons,[15,42,43] increases almost linearly with charge, attains the maximum at ca. 2 F mol^{-1}, and then decreases, tending to zero at 4 F mol^{-1}. The maximum conductivity is comparable with that of I_2-doped tetradecyldodecathiophene (5 S cm^{-1}).[36]

Evolution of Conductivity with Doping. The conduction in a series of polypyrroles and polythiophenes[15,42,43] and in a regioregular polythiophene[44] has been previously examined in situ as a function of the doping charge. The results

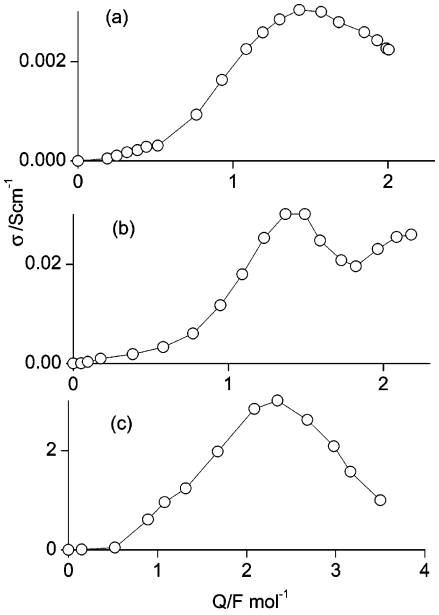

Figure 10. In situ conductivity vs charge of (a) CA2H4T8, (b) H6T10, and (c) Br2H8T12 films in acetonitrile + 0.1 M Bu_4NClO_4.

obtained there help in understanding the behavior of the oligothiophenes investigated here.

The evolution of the conductive properties in sexithiophenes as a function of the oxidation degree may be explained as follows. Oxidation produces polarons which are expected to be confined right in a hexameric segment.[45,46] Here they are strongly π-dimerized,[38] and the materials are insulating.[15,42,43,44] Further oxidation produces bipolarons, and their confinement in the same hexameric unit again produces an insulating state. Conduction is anyway obtained as a mixed-valence one from polarons either with bipolarons (polaron−bipolaron conduction) or with undoped states (neutral−polaron conduction) as previously reported for a long series of sexithiophene films.[5]

The difluorenonyl- and difluorenylsexithiophenes show in fact a clear polaron−bipolaron redox conduction, but the further conductive state beyond the two-electron oxidation has no redox characteristics. At a high doping level a lattice of strongly π-interacting chains, providing electron-filled states available for conduction, is obtained. The observed conductive behavior is that expected for free charges hopping within a potential range with a constant density of states (metal-like conduction).[47] The metal-like conductivity at the higher doping level is ca. 20-fold higher than the polaron−bipolaron conductivity, which is in its turn ca. 10-fold higher than the neutral−polaron conductivity.[5] Thus, conductivity increases exponentially with each oxidation step.

In the octathiophene the two extra thiophene rings do not bring about an increase of the allowed doping charge, which remains at the level of 2 F mol^{-1} at the same switching potential, but change the cyclic voltammogram from a redox to a capacitive one, with only signs of redox processes. The

(41) Bauerle, P. *Adv. Mater.* **1992**, *4*, 102.
(42) Zotti, G.; Schiavon, G.; Zecchin, S.; Berlin, A. *Synth. Met.* **1998**, *97/3*, 245.
(43) Zotti, G.; Zecchin, S.; Schiavon, G.; Vercelli, B.; Berlin, A.; Dalcanale, E.; Groenendaal, L. *Chem. Mater.* **2003**, *15*, 4642.
(44) Kunugi, Y.; Harima, Y.; Yamashita, K.; Ohtab, N.; Ito, S. *J. Mater. Chem.* **2000**, *10*, 2673.
(45) Navarrete, J. T.; Zerbi, G. *J. Chem. Phys.* **1991**, *94*, 965.
(46) Christensen, P. A.; Hamnett, A.; Hillman, A. R.; Swann, M. J.; Higgins, S. J. *J. Chem. Soc., Faraday Trans.* **1992**, *88*, 595.
(47) Focke, W. W.; Wnek, G. E. *J. Electroanal. Chem.* **1988**, *256*, 343.

conductivity values are almost the same as those of the sexithiophene.

In the decathiophene the four extra thiophene rings start producing an increase of charge, which anyway remains at the maximum level of 2.3 F mol^{-1} at the same switching potential, but change the cyclic voltammogram to a fully capacitive one. The maximum conductivity undergoes a 10-fold increase compared with that of the octathiophene.

These results, which confirm those previously obtained for Me2T8 and Me2T10,[40] can be explained if we assume that bipolarons, which were pinned in the sexithiophene moiety, can now delocalize over two to four extra thiophene rings. As a consequence the two-electron-oxidized octamer and (to a higher extent) the decamer also display capacitive properties, attributable to the availability of electron-filled states of approximately constant density.

In the dodecathiophene, expanding further the oligothiophene chain length (doubling the thiophene rings) increases strongly the allowed redox charge to values approaching 4 F mol^{-1} and the cyclic voltammogram becomes a simple flat capacitive response. Here the conduction increases with charge and then decreases to complete the depletion of the valence band in the tetracation. Moreover, the conductivity is strongly enhanced, attaining values even 100 times higher than in the decathiophene. This impressive increase of conductivity from the decamer to the dodecamer may be related to the huge increase of the allowed doping level.

Bipolarons are also the carriers in this case. Like bipolarons are confined in a hexameric segment; the tetracationic charge is localized in the dodecathiophene chain, making it insulating, but bipolarons are free to move at lower levels of doping. 3D hopping of bipolaron charges within and between adjacent polymer chains has been described as a concerted transfer of the twin bipolaron charge to a bipolaron-free polymer segment.[48] In this model the presence of both bipolaron-carrying and bipolaron-free segments is required for conduction, and this therefore results in a redox-like[39] conduction with a maximum at the two-electron-oxidized state.

To summarize, both heterogeneous (e.g., fluorenone or fluorene) and homogeneous (thiophene) extensions of conjugation increase the allowed doping charge level and conductivity of sexithiophenes. However, in the former case, charge injection is localized at the sexithiophene core first and only at high charges is delocalization over the whole conjugated chain obtained. In all cases, high doping charges are stored in a capacitive fashion and the relevant conductivity is metal-like.

Conclusions

Extending the conjugation beyond the sexithiophene frame with long molecular fragments gives novel electronic and conductive properties to the molecular wire.

Thin solid films of regular hexyl-substituted sexithiophenes, fluorenonyl- and fluorenyl-substituted at the terminal α,ω-positions, and of hexyl-substituted α,ω-capped octathiophene, decathiophene, and dodecathiophene were electrochemically modulated, and their conductivity was investigated by in situ measurements. The dodecathiophene represents the longest regular oligothiophene ever investigated electrochemically in the solid state.

In sexithiophenes the reversible oxidation is composed of three separate steps, two one-electron processes and a further multielectron process. Conductivity is redox type at the cation−dication (polaron−bipolaron) state and metal-like at the subsequent oxidation state with a 20-fold increase at full oxidation. Capacitive properties are displayed early at levels lower than the one-electron oxidation state.

In the α,ω-capped octathiophene, decathiophene, and dodecathiophene oxidation occurs in a single process with extended capacitive properties. Conductivity, which increases progressively (by 3 orders of magnitude) with the oligothiophene chain length, is metal-like in all cases. It is noteworthy that in dodecathiophene (twice the sexithiophene) the maximum allowed doping charge approaches four electrons per molecule and the conductivity, maximized at the two-electron level, decreases linearly, approaching zero at the four-electron level. A bipolaron model accounts for conductivity in oligothiophenes.

Comparing the results reported here for the fluorenonyl- and fluorenyl-substituted sexithiophenes with those for the capped sexithiophenes presented in part 1 of this series,[5] we can observe that sexithiophene is in all cases the location of the first two-electron oxidation, further oxidation and related conduction being allowed by extensively conjugated end moieties.

The results obtained are of fundamental importance for the understanding of the basic conductivity of these materials as models of conducting polymers. Moreover, they will be particularly useful for the analysis of the conductive properties of conjugated molecular wires.

Acknowledgment. We thank Dr. R. Seraglia of ISTM-CNR for obtaining the MALDI spectra, Dr. G. Schiavon of IENI-CNR for helpful discussions, and S. Sitran of IENI-CNR for his technical assistance.

CM060671H

(48) Chance, R. R.; Bredas, J. L.; Silbey, R. *Phys. Rev. B* **1984**, *29*, 4491.